

Eccentric binary neutron star mergers

Roman Gold,^{1,2} Sebastiano Bernuzzi,¹ Marcus Thierfelder,¹ Bernd Brügmann,¹ and Frans Pretorius²

¹*Theoretisch-Physikalisches Institut, Friedrich Schiller Universität Jena, Max-Wien-Platz 1, 07743 Jena, Germany*

²*Department of Physics, Princeton University, Princeton, NJ 08544, USA.*

(Dated: September 26, 2011)

Neutron star binaries offer a rich phenomenology in terms of gravitational waves and merger remnants. However, most general relativistic studies have been performed for nearly circular binaries, with the exception of head-on collisions. We present the first numerical relativity investigation of mergers of eccentric equal-mass neutron-star binaries that probes the regime between head-on and circular. In addition to gravitational waves generated by the orbital motion, we find that the signal also contains a strong component due to stellar oscillations (f -modes) induced by tidal forces, extending a classical result for Newtonian binaries. The merger can lead to rather massive disks on the order of 10% of the total initial mass.

Introduction. Binary neutron star (NSNS) mergers are among the most promising sources of gravitational waves (GWs) for ground-based interferometers, as well as plausible candidates for the central engine of short-gamma-ray-burst (sGRB). One of the main tools to study NSNS mergers is numerical relativity, which experienced a dramatic development in the last 10 years achieving important results in NSNS [1–3] and recently also for black hole-neutron star (BHNS) simulations [4, 5]

In numerical relativity NSNS mergers have been almost exclusively studied for circularized initial data, with the exception of head-on collisions [6, 7] (and see [8] for a nearly head-on Newtonian simulation with radiation reaction). Somewhat surprisingly, there are no numerical studies of orbits with eccentricity (discounting the residual eccentricity [9] of quasi-circular data). One reason for this is an expectation that the dominant population of NSNS mergers in the universe results from evolution of primordial stellar binaries. For such systems, residual eccentricity at the time of merger is expected to be low. For example, a recent investigation suggests that only between 0.2% and 2% of this class of mergers detectable by Advance LIGO/VIRGO will have eccentricity $e > 0.01$ (and $e \lesssim 0.05$) [10]. With such small residual eccentricity quasi-circular templates will be able to detect the majority of these events [11], and moreover templates have been proposed for weakly eccentric binaries ($e \lesssim 0.10$) [12]. However, recent studies have suggested there may be a significant population of compact object binaries formed via dynamical capture in dense stellar environments [13, 14]. In [14], it is estimated that the rate of dynamical capture NSNS mergers may be large enough to account for a significant fraction of sGRBs, assuming NSNS mergers are their progenitors. Observations of sGRBs have also suggested there are different progenitors for sGRBs that exhibit so called extended emission and those that do not [15]; an obvious speculation of the cause of the bimodality is primordial vs. dynamical capture NSNS mergers. A large fraction of this latter class of mergers will occur with high eccentricity.

Eccentric mergers can lead to a rich phenomenology in the GW and the merger remnant. The properties of the accretion disk formed as a product of the merger are so

far poorly understood, even though there is the possibility of massive disk production, $M_d \sim 10\%$ of the total initial binary mass. Recent results [16] for BHNS systems indicate a strong variability in properties of the merger remnant as a function of the eccentricity. The gravitational waveforms significantly differ from the chirp signal of quasi-circular inspirals that feature slowly increasing amplitude. During eccentric orbits, each periastron passage leads to a burst of radiation, first studied using Newtonian orbits together with leading order relativistic expressions for radiation and evolution of orbital parameters [17, 18], and more recently with numerical simulations of BHBH and BHNS systems in full general relativity [16, 19–21]. An important Newtonian result concerning NSNS (or BHNS) is that eccentricity leads to tidal interactions that can excite oscillations of the stars, which in turn generate their own characteristic GW signal [22] (see also [23, 24]). In some cases the GWs can be dominated by these non-orbital contributions [22]. Neither the orbital nor stellar GWs have been studied so far for eccentric NSNS orbits in general relativity.

In this letter we present the first numerical relativity investigation of (highly) eccentric NSNS mergers. We consider an equal-mass binary at fixed initial separation and vary the initial eccentricity. Three models are discussed that are representative of the different orbital phenomenology observed: direct plunge, merger after a close encounter, multiple encounters. We analyze the emitted GW, the dynamics in the matter and characterize the basic properties of the merger remnant. Dimensionless units $c = G = M_\odot = 1$ are used if not stated otherwise.

Numerical Method. We performed numerical simulations in 3+1 numerical relativity solving the Einstein equations coupled to a perfect fluid matter model (no magnetic fields). We employed the BAM code [25, 26], which we recently extended to general relativistic hydrodynamics [27]. Referring to [26, 27] for details and further references, we solve the BSSN formulation in the moving puncture gauge coupled to matter in flux-conservative form. Metric and matter fields are discretized in space on 3D Cartesian meshes refined with the technique of moving boxes. Time integration is performed with the method-of-lines using a 3rd order Runge-Kutta scheme.

Derivatives of metric fields are approximated by fourth-order finite differences, while a high-resolution-shock-capturing scheme based on the local-Lax-Friedrich central scheme and the convex-essentially-non-oscillatory reconstruction is adopted for the matter. Neutron star matter is modeled with a polytropic equation of state with adiabatic index $\Gamma = 2$. Gravitational waveforms are extracted at finite coordinate radius, $r \sim 90M$, by using the Newman-Penrose curvature scalar, Ψ^4 , where $M = 2.8M_\odot$ is the gravitational mass of the system.

Although the problem of posing initial data to the Einstein equations by solving the constraints is in principle well understood, there is no ready-made prescription for eccentric NSNS that are of interest here. We postpone the solution of the constraint equations and instead work with the following approximation. Initial data are set by superposing two boosted non-rotating stars with the same gravitational mass $1.4M_\odot$ at apoastron. The two stars are located at coordinates $(x_\pm, y, z) = (\pm 25M, 0, 0)$ and boosted with parameters $\xi_\pm = (0, \pm \xi_y, 0)$, respectively. The initial data are asymptotically flat but not conformally flat, and approximately irrotational. The maximum constraint violation (at the center of the star) decays as $1/d$ as expected for the relatively large initial proper separation $d \sim 54.7M$. The constraint violation is at the level of the truncation error of the evolution scheme (see also the discussion in [16]).

Orbital dynamics. We performed a series of simulations for different initial boosts (i.e. Newtonian apoastron velocities), $\xi_y \in [0.01, 0.05]$. Newtonian circular orbits are obtained for $\xi_y \simeq 0.07$. The grid configuration consisted of five refinement levels, maximum spatial resolution $h \sim 0.1 - 0.2M_\odot$ and a Courant-Friedrichs-Levy factor of 0.25. For $\xi_y \lesssim 0.020$, within $1000M$ a merger and formation of a black hole occurred. Selected models were continued for $\sim 10ms$ after the merger in order to follow the accretion process onto the final black hole. During evolutions the largest violation of the rest-mass conservation occurs before collapse $\Delta M_0/M_0 \sim 0.01$. Similarly the ADM mass was conserved up to 1%. The consistency of the results was assessed by convergence tests.

We begin by reporting the orbital dynamics in our three models. See Fig. 1 for the star tracks as computed from the minimum of the lapse function [27].

In Model 1 ($\xi_y = 0.010$) the stars move almost directly towards each other, collide, then undergo prompt collapse to a black hole at $t - r = 423M$ with dimensionless spin parameter $a_{\text{BH}} \sim 0.58$ and mass $M_{\text{BH}} \sim 2.8M_\odot$. The resulting disk has negligible rest-mass, $M_d \lesssim 10^{-7}M_0$, which is at the level of the artificial atmosphere used for the numerical treatment of vacuum for the matter.

In Model 2 ($\xi_y = 0.020$) the stars come in contact but survive the first encounter. During contact matter is exchanged between the outer layers of the stars, see Fig. 2, which in turn gain rotation; the density weighted Newtonian vorticity is 10 times larger than an irrotational NSNS binary. During a second encounter they merge forming a black hole at $t = 975M$ with initial $a_{\text{BH}} \sim 0.79$

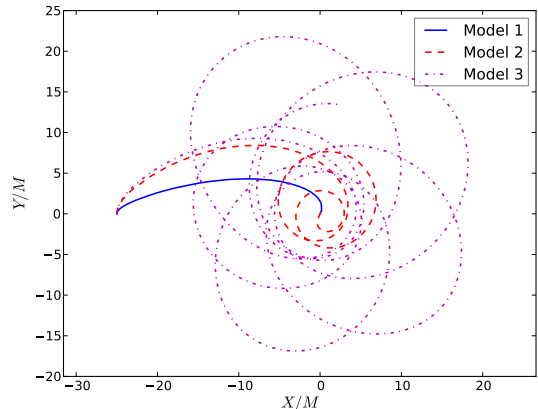


FIG. 1: Star tracks for Model 1, 2, and 3. The tracks of the second star can be inferred from symmetry.

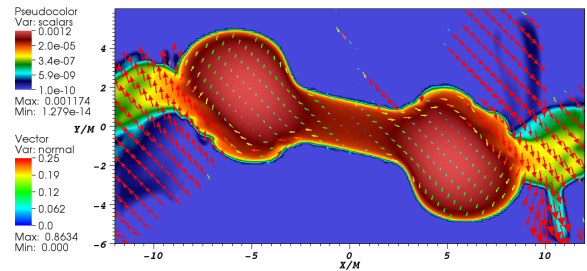


FIG. 2: Model 2 at $t = 523M$, shortly after the stars have touched and separated again. The rest-mass density (log-scale) and the three-velocity in the orbital plane are shown.

and mass $M_{\text{BH}} \sim 2.2M_\odot$. In contrast to Model 1, there is a massive disk with $M_d \sim 0.08M_0 \sim 0.15M_\odot$, measured $100M$ after the formation of an apparent horizon; meanwhile accretion has increased the mass and spin to $M_{\text{BH}} \sim 2.64M_\odot$ and $a_{\text{BH}} \sim 0.81$. At the onset of merger, the separation remains nearly constant $\sim 5M$. This suggests a transition through a whirl regime as was observed in BBH systems [16, 19–21, 28]. We stress, however, that the binary is in contact at this point and that the matter interaction may lead to additional effects. After the merger we observe quasi-periodic oscillations in the accretion flow at a frequency $\nu_{\text{QPO}} \sim 0.5kHz$ in the vicinity of the black hole.

In Model 3 ($\xi_y = 0.022$) multiple close passages with no matter exchange are observed. The two bodies do not merge during a simulation time of $t = 5400M$. The orbits show a significant periastron precession, leading to an overall rotation of the quasi-elliptical orbit of almost 90 degrees per encounter. However, zoom-whirl orbits are unstable, which suggests that by $t = 5400M$ Model 3 has not yet quite evolved to this regime.

Waveforms. The orbital motion of each model results in a characteristic gravitational wave signal. Figs. 3 and 4 display the $\ell = m = 2$ mode, Ψ_{22}^4 , as well as the corresponding instantaneous gravitational wave frequency,

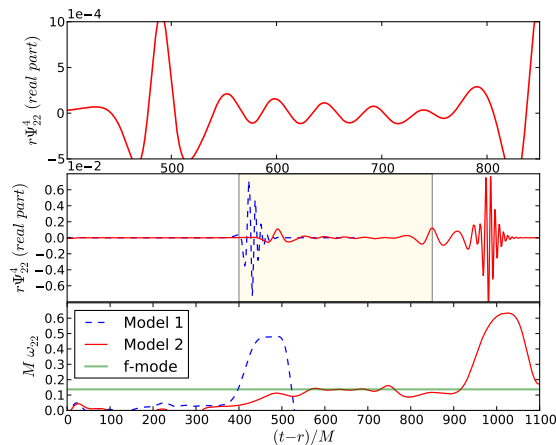


FIG. 3: Real part of the $r\Psi_{22}^4$ waveforms (central panel) and instantaneous gravitational wave frequency (bottom panel), $M\omega_{22}$, as a function of retarded time, $(t-r)/M$, for Models 1 and 2. The top panel shows a zoom in on the shaded region in the central panel for Model 2. The horizontal line in the bottom panel marks the perturbative f -mode frequency.

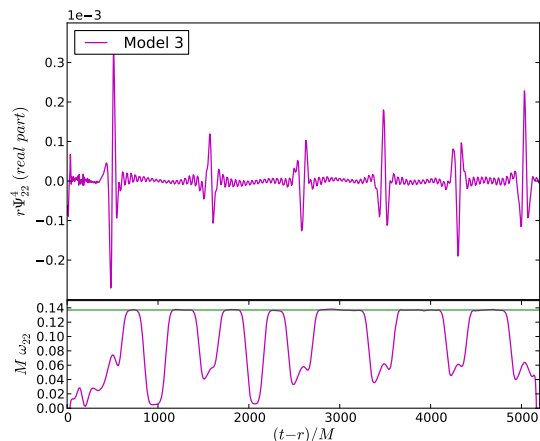


FIG. 4: Same as the central and bottom panels of Fig. 3 but for Model 3.

$M\omega_{22}$, of the curvature scalar, which represents the main emission channel for the binary signal.

Waveforms from Model 1 are characterized by a peak at the merger and the subsequent quasi-normal-mode (QNM) ringing of the final black hole. The GW frequency of the QNM is $M\omega_{22} \sim 0.48$, compatible with the fundamental QNM frequency of the Kerr black hole computed from the apparent horizon parameters, e.g. [29]. In fact, we find the value $\nu_{\text{QNM}} \sim 5.9 \text{ kHz}$, which differs by 6% from the value obtained from the GW. Waveforms from Model 2 show a burst at retarded time $t-r \sim 500M$ related to the orbital dynamics [18], followed by a feature between $t-r \sim [800M - 900M]$ akin to a transition through a whirl phase and the final merger signal around $t-r \sim 1000M$. In this case the QNM frequency is higher, $M\omega_{22} \sim 0.632$ ($\nu_{\text{QNM}} \sim 7.6 \text{ kHz}$, 2%

discrepancy). The waveforms from Model 3 exhibit several bursts corresponding to the periastron passages.

The key feature is that between the bursts, (see e.g. for Model 2 at $t-r \sim [550 - 750M]$). One can observe high frequency signals in several GW-modes, which are absent in the black hole case, but qualitatively similar to BHNS eccentric mergers [16]. This signature is progressively suppressed at lower eccentricities (larger ξ_y) and not observed for $\xi_y = 0.05$. Referring to Fig. 4, the $(2, 2)$ GW frequency is dominated by several plateaus compatible with the f -mode frequency of the non-rotating star in isolation [30–32], $M\omega_f \sim 0.137$ ($\nu_f \sim 1.586 \text{ kHz}$), interrupted briefly by the close encounter bursts (the interruptions at $t \sim 1000M, 2000M$ disappear for larger extraction radii). In Model 2, the signal is mainly in the $(2, 2)$ multipole; the $(2, 0)$ multipole (not shown) also contains the signature (weaker in amplitude by a factor five). In contrast, in Model 3 the amplitude of the $(2, 2)$ multipole is smaller in amplitude by a factor of three than the $(2, 0)$ multipole, which is the main emission channel between the bursts (encounters).

The natural interpretation is that these GWs are produced by oscillations of the individual stars, which are tidally induced by the companion. Physically, the expectation is that the approximately head-on, zoom-part of the orbit is responsible for exciting axisymmetric $m = 0$ modes, while in particular $m = 2$ modes should arise from the approximately circular, partial whirl near apoastron. The relative amplitude of the modes indicates the effectiveness of the different phases of the binary interaction to excite certain modes. Indeed the Newtonian analysis of Turner [22] indicates that a sufficiently close periastron passage (i.e. $e \lesssim 1$ for fixed apoastron) exerts a pulse-like tidal perturbation which excites the axisymmetric f -modes of the star, leading to a GW waveform dominated by the star oscillations rather than by the emission due to the orbital motion. Note that the phenomenon is different from a resonant tidal excitation, see e.g. [23, 33], which instead refer to the circular motion case.

If these waves indeed correspond to stellar f -modes, they should be detectable as oscillations of the stellar matter. A way to identify the modes is to consider the projections of the rest-mass density of one of the stars onto the spherical harmonics, e.g. [31], $\rho_{\ell m} \equiv \int Y_{\ell m}^* \rho d^3x$, and perform an analysis of the spectrum. Results are reported in Fig. 5 for Model 2 and 3, where the $\rho_{22}(t)$ projections and their power spectral density (PSD) are shown. In both models we can clearly identify frequencies compatible with the linear f -mode (broadened by the signal length in Model 2), together with secondary peaks eventually due to nonlinear couplings. Similar results are obtained for the axisymmetric ($m = 0$) quadrupole mode, while in this case the signal is strongly modulated by the orbital motion. Overall the analysis indicates that both non-axisymmetric and axisymmetric f -modes are excited during the encounter. Note that, given an uncertainty on the frequencies, we can estimate an upper limit on the rotation of the star. In model 3 there are

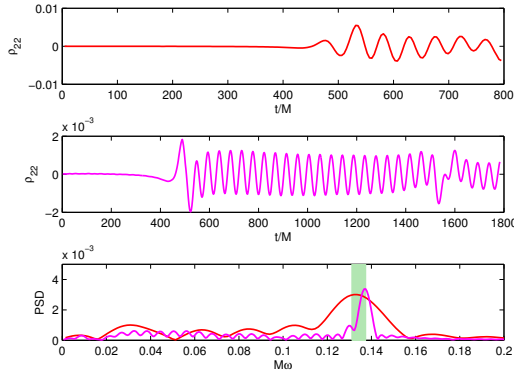


FIG. 5: Mode analysis. The panels display the $\ell = m = 2$ spherical-harmonic projection of the rest-mass density of one of the stars (Model 2 top, Model 3 center), and its power spectral density (PSD, bottom), where ν_f is marked. The width of the green shaded area, 73Hz , spans the perturbative values of the mode frequencies of models A0-A5 (right-left).

more cycles leading to the most restrictive estimate for the maximum rotation rate (rotational energy/potential energy) of ~ 0.05 , i.e. at most mildly rotating [30]. r -

modes are thus not expected, but they may be present in the outer layers of Model 2; g -modes are absent here by construction.

Conclusion. Mergers of eccentric NSNS could be very interesting sources for third generation GW detectors, in particular given the (in some respect) surprisingly strong and clear signal from orbit-induced stellar oscillations (OISOs). If detected, this would pose constraints on the equation of state. The present results are likely to be highly dependent on the compactness of the stars and on the mass ratio, thus these cases should be studied as well. Furthermore, even larger disk masses are expected for the unequal mass case which could be interesting for sGRB astrophysics. More work is required in these directions together with a detailed understanding of the eccentric NSNS distribution in the Universe.

Acknowledgments. We gratefully acknowledge helpful discussions with William East, Branson Stephens and Kostas Kokkotas. This work was supported in part by DFG SFB/Transregio 7. RG was supported by DFG GRK 1523, in particular during a stay at Princeton, FP was supported by NSF grant PHY-0745779 (FP) the Alfred P. Sloan Foundation. Computations were performed on JUROPA (Jülich) and at the LRZ (Munich).

-
- [1] J. A. Font, Living Reviews in Relativity **11** (2008).
 - [2] J. A. Faber, T. W. Baumgarte, S. L. Shapiro, and K. Taniguchi, Astrophys. J. Lett. **641**, L93 (2006), astro-ph/0603277.
 - [3] L. Rezzolla, B. Giacomazzo, L. Baiotti, J. Granot, C. Kouveliotou, and M. A. Aloy (2011), 1101.4298.
 - [4] M. Shibata and K. Taniguchi, Living Reviews in Relativity **14** (2011).
 - [5] M. D. Duez, Class. Quant. Grav. **27**, 114002 (2010), 0912.3529.
 - [6] K.-J. Jin and W.-M. Suen, Phys. Rev. Lett. **98**, 131101 (2007), gr-qc/0603094.
 - [7] T. Kellermann, L. Rezzolla, and D. Radice, Class. Quant. Grav. **27**, 235016 (2010), 1007.2797.
 - [8] M. Shibata, T. Nakamura, and K. Oohara, Prog. Theor. Phys. **89**, 809 (1993).
 - [9] M. Miller, Phys. Rev. D **69**, 124013 (2004), gr-qc/0305024.
 - [10] I. Kowalska, T. Bulik, K. Belczynski, M. Dominik, and D. Gondek-Rosinska, Astron. Astrophys. **527**, A70 (2011), 1010.0511.
 - [11] K. Martel and E. Poisson, Phys. Rev. **D60**, 124008 (1999), gr-qc/9907006.
 - [12] T. Cokelaer and D. Pathak, Class. Quant. Grav. **26**, 045013 (2009), 0903.4791.
 - [13] R. M. O’Leary, B. Kocsis, and A. Loeb, MNRAS **395**, 2127 (2009), 0807.2638.
 - [14] W. H. Lee, E. Ramirez-Ruiz, and G. van de Ven, Astrophys. J. **720**, 953 (2010), 0909.2884.
 - [15] J. P. Norris, N. Gehrels, and J. D. Scargle, Astrophys. J. **735**, 23 (2011), * Temporary entry *, 1101.1648.
 - [16] B. C. Stephens, W. E. East, and F. Pretorius, Astrophys. J. **737**, L5 (2011), 1105.3175.
 - [17] P. C. Peters and J. Mathews, Phys. Rev. **131**, 435 (1963).
 - [18] M. Turner, Astrophys. J. **216**, 610 (1977).
 - [19] F. Pretorius and D. Khurana, Class. Quant. Grav. **24**, S83 (2007), gr-qc/0702084.
 - [20] U. Sperhake, E. Berti, V. Cardoso, J. A. Gonzalez, B. Brügmann, and M. Ansorg, Physical Review D **78**, 064069 (2008), URL doi:10.1103/PhysRevD.78.064069.
 - [21] R. Gold and B. Brügmann, Class. Quantum Grav. **27** (2009), 0911.3862.
 - [22] M. Turner, Astrophys. J. **216**, 914 (1977).
 - [23] K. D. Kokkotas and G. Schäfer, Mon. Not. Roy. Astron. Soc. **275**, 301 (1995), gr-qc/9502034.
 - [24] W. H. Lee, E. Ramirez-Ruiz, and G. van de Ven, Astrophys. J. **720**, 953 (2010), 0909.2884.
 - [25] B. Brügmann, W. Tichy, and N. Jansen, Phys. Rev. Lett. **92**, 211101 (2004), gr-qc/0312112.
 - [26] B. Brügmann, J. A. González, M. Hannam, S. Husa, U. Sperhake, and W. Tichy, Phys. Rev. **D77**, 024027 (2008), gr-qc/0610128.
 - [27] M. Thierfelder, S. Bernuzzi, and B. Brügmann, Phys. Rev. D **84**, 044012 (2011), arXiv:1104.4751.
 - [28] J. Healy, J. Levin, and D. Shoemaker, Phys. Rev. Lett. **103**, 131101 (2009), 0907.0671.
 - [29] F. Pretorius (2007), arXiv:0710.1338v1 [gr-qc].
 - [30] H. Dimmelmeier, N. Stergioulas, and J. A. Font, Mon. Not. Roy. Astron. Soc. **368**, 1609 (2006), astro-ph/0511394.
 - [31] L. Baiotti, S. Bernuzzi, G. Corvino, R. De Pietri, and A. Nagar, Phys. Rev. **D79**, 024002 (2009), 0808.4002.
 - [32] E. Gaertig and K. D. Kokkotas, Phys. Rev. **D83**, 064031 (2011), 1005.5228.
 - [33] W. C. G. Ho and D. Lai, Mon. Not. Roy. Astron. Soc. **308**, 153 (1999), astro-ph/9812116.